Compumag 2011

12 - 15 July 2011, Sydney, Australia

18th International Conference on the Computation of Electromagnetic Fields

(www.compumag2011.com)

TECHNICAL PROGRAM

(Draft on 22 June 2011)

PB10.13 (ID 633)
Driving Characteristics of an HTS Linear Synchronous Motor for an HTS Magnetic Suspension and Propulsion System
Jin, Jian-Xun (1); Zheng, Lu-Hai (1); Xu, Wei (2); Guo, You-Guang (2); Zhu, Jian-Guo (2)
1: School of Automation, University of Electronic Science and Technology of China, Chengdu, China; 2: Faculty of Engineering and Information Technology, University of Technology Sydney, Sydney, Australia

PB10.14 (ID 630)
Finite Element Analysis and Evaluation of Stator Insulation in High Voltage Synchronous Motor
Zhang, Jun (1); Li, Haibo (1); Wang, Shuhong (1); Qiu, Jie (1); Zhu, Jian Guo (2); Guo, Youguang (2)
1: Xi'an Jiaotong University, China, Peoples Republic of; 2: University of Technology, Sydney, Australia

PB10.15 (ID 635)
Analysis of Interior Permanent Magnet Synchronous Motor on Electromagnetic Vibration
Sun, Tao; Lee, Jae-Min; Lee, Byeong-Hwa; Kim, Hea-Joong; Hong, Jung-Pyo
Hanyang University, Korea, South (Republic of)

PB10.16 (ID 439)
Analysis of Novel Brushless DC Motors Made of Soft Magnetic Composite
Ishikawa, Takeo; Takahashi, Kazutoshi; Ho, QuangViet; Matsunami, Michio; Kurita, Nobuyuki
Gunma University, Japan

Session PB11: Wave Propagation and EMC (III)

16:15-17:30 – Bayside Gallery

PB11.1 (ID 109)
Fast and Accurate Prediction of Reverberation Chambers' Resonant Frequencies Using Time-Domain Integral Equation and Matrix Pencil Method
Zhao, Huapeng; Shen, Zhongxiang
Nanyang Technological University, Singapore

PB11.2 (ID 193)
A Full PEEC Modeling of EMI Filter Inductors in Frequency Domain
Kovacevic, Ivana; Friedli, Thomas; Musing, Andreas; Kolar, Johann
Swiss Federal Institute of Technology, Switzerland

PB11.3 (ID 200)
Application of Chaotically Frequency Modulated SVPWM for EMC Enhancement of Closed-loop Motor Drives
Wang, Zheng; Chau, K. T.; Cheng, M.; Ding, Shichuan
Southeast University, China, Peoples Republic of

PB11.5 (ID 224)
Transmission Line Modeling Method Applied to Evaluate Effective Length of Impulsive Grounding Electrodes
Gazzana, Daniel da Silva (1); Bretas, Arturo Suman (1); Dias, Guilherme Alfredo D. (1); Telló, Marcos (2)

> CMP-635<

A study on the estimated method of vibration in Interior Permanent Magnet Synchronous Motor

Do-Jin Kim, Tao Sun, Hae-Joong Kim, Jae-Min Lee, and Jung-Pyo Hong

Department of Automotive Engineering, Hanyang University, Haengdang-dong, Seongdong-gu, Seoul 133-791, Korea

Using a numerical process, this paper analyzes the vibration of interior permanent magnet synchronous motor (IPMSM) due to the electromagnetic force. This process includes calculation of local force in electromagnetic finite element analysis (FEA), and estimation of natural frequency and deformation in mechanical structural analysis. Additionally, the harmonic components are analyzed from the radial force in the air gap. The effects of local force which is calculated on surface of tooth and electromagnetic force are investigated according to the analysis results. Two IPMSM models which have the same characteristics but different stator structures will be studied. The calculated results will be validated by an experiment.

***Index Terms*—Numerical analysis, Equivalent magnetizing current, Maxwell stress tensor, Harmonic spectrum**

I. Introduction

Interior permanent magnet synchronous motor (IPMSM) has been employed in various devices, such as wash machine, air conditioner, electric scooter, and hybrid electric vehicle. These devices surrounding people has highly demanding requirement on the vibration, because that the vibration does not only cause the vibro-noise, but also reduce the useful life of the devices.

In the electric motor, the vibration is mainly excited by the electromagnetic force which is consists of the tangential component and radial component. Many literatures proposed the estimation methods for the vibration of electric motor by analyzing the electromagnetic force. These methods generally can be divided into the total force analysis method and the local force analysis method. In the total force analysis method [1]-[2], the tangential component of electromagnetic force is ignored, and only the radial component of electromagnetic force in the air gap of motor is calculated. By using the harmonic analysis, e.g. Fast Fourier Transform (FFT) analysis, the harmonic order and amplitude of the radial force then is obtained. Due to the calculation in the air gap, the total force can not be used to the structural analysis. Therefore, the total force analysis method usually studies if there is the frequency of the radial force is close to one of the natural frequencies of the stator when the force order is the same as the circumferential vibrational mode of the stator. It is obvious that the total force analysis method only considers the worst condition of vibration but can not give the specific value.

In order estimate the vibration of motor, both the tangential component and radial component of electromagnetic force acting on each stator tooth should be calculated, i.e. the local force analysis. Vandevelde *et al.* [3] compared equivalent magnetization method and virtual work on the force calculation in a switched reluctance motor, and demonstrated that the validity of the equivalent magnetization method on the deformation analysis. But only the force calculation was discussed rather than the vibration characteristics. Using the Maxwell stress tensor method and equivalent magnetization method, Chen *et al.* [4] and Lee *et al.* [5] calculated the local force and successfully estimated the vibration in the permanent magnet synchronous motor, respectively.

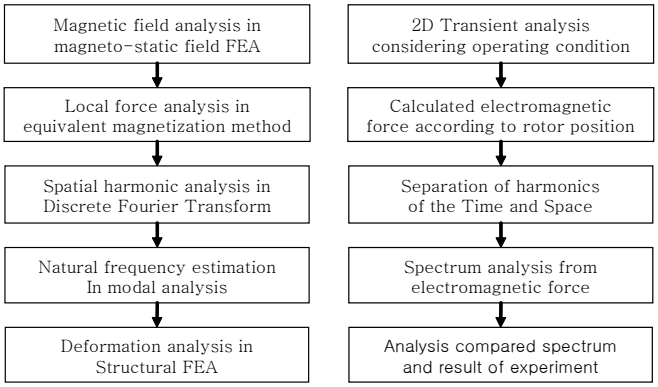

Fig. 1. Process of estimated vibration

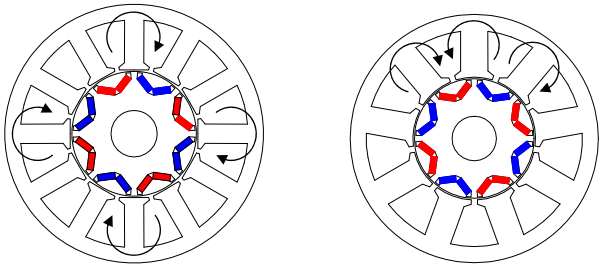

(a) (b)

Fig. 2. Cross-sections of the study IPMSM models: (a) 8-pole/12-slot model; (b) 8-pole/9-slot model.

However, the relationship between the local force and the vibration was not revealed. Additionally, due to the special rotor structure, there is no analytical model which can accurately calculate total force or local force in IPMSM model.

Based on this background, this paper analyzes the vibration of IPMSM due to the electromagnetic force by using a numerical process. As shown in Fig. 1, this process 1 includes the electromagnetic finite element analysis (FEA), local force calculation, modal analysis, deformation analysis and harmonic analysis. The effects of local force which is calculated on surface of tooth and electromagnetic force are investigated according to the analysis results. In process 2, in order to analyze slot harmonic components, the electromagnetic force which is calculated from air gap flux density is analyzed according to time and space. Two

TABLE I
SPECIFICATION OF STUDY MODELS

Item	Value	
	8/12 model	8/9 model
Rated power [kW]	2	
DC link voltage [V]	42	
Rated current [A_{rms}]	52	58
Maximum torque [Nm]	5.5	
Stator/rotor outer diameter [mm]	100.4 / 48.4	
Stack length / air gap [mm]	95 / 0.6	

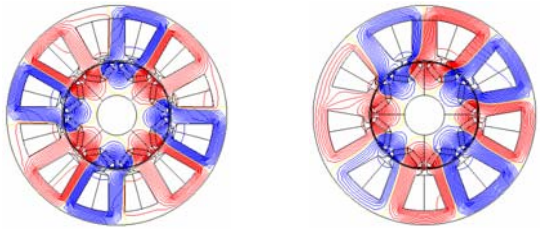

(a) (b)

Fig. 3. Flux distribution of the study models in the load condition: (a) 8-pole and 12-slot model; (b) 8-pole and 9-slot model.

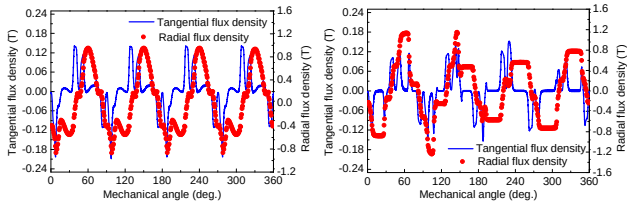

(a) (b)

Fig. 4. Tangential and radial flux densities: (a) flux density of 8-pole and 12-slot model; (b) flux density of 8-pole and 9-slot model.

IPMSM models which have the same characteristics but different stator structures are studied by this process. Finally, the calculated results are verified by an experiment.

II. Study Models

The cross-sections of two IPMSMs are shown in Fig. 2. They have the identical rotor structure but different stator. The combination of pole and slot of one model is 8/12. The other has the 8/9 combination of pole and slot, i.e. the structure that slot number (N_s) and pole number (N_p) differ by one (N_p=N_S+1). The specifications of these two models are listed in Table I.

III. Electromagnetic Force Calculation

Fig. 3 shows the flux distribution of the study models in the load condition (i_d=0). It can be seen that the flux distribution in the 8-pole/9-slot model is obviously asymmetrical. In the same load condition (3.5Nm), the tangential and radial components of flux density in the air gap of these two models are calculated and shown in the Fig. 4. It is observed that both the tangential and radial components of the flux density of 8-pole/12-slot model are spatially periodic, while the flux densities of 8-pole/9-slot model are nonperiodic.

In order to verify the effect of the symmetrical and asymmetrical radial forces on the vibration, the local force acting on the stator tooth is required [5]. Compared with the

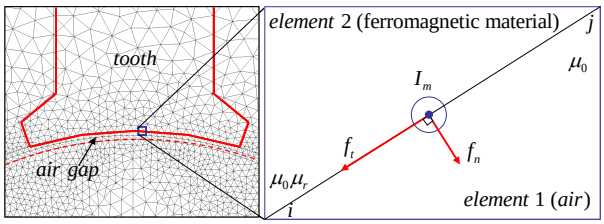

Fig. 5. Equivalent magnetizing current in the boundary line.

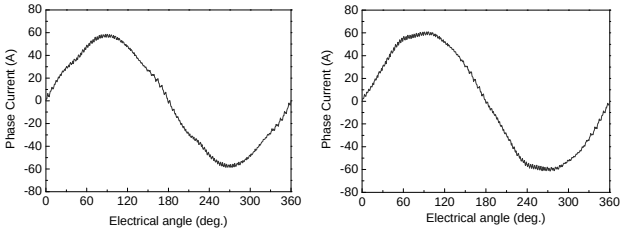

(a) (b)

Fig. 6. Experiment current waveforms for the local force calculation: (a) 8-pole/12-slot model; (b) 8-pole/9-slot model.

Maxwell stress tensor method and virtual work method, [6] demonstrated that the equivalent magnetizing current method is the more accurate method to calculate the local force. Fig. 5 indicates the equivalent magnetizing current between two elements with different materials. It can be obtained in

$$I_m = \frac{1}{\mu_0}\int(\nabla\times\boldsymbol{M})\cdot d\boldsymbol{s} = \frac{1}{\mu_0}(M_{1t}-M_{2t})l_{ij} \qquad (1)$$

where M_{1t} and M_{2t} are the tangential components of the intensity of magnetization on the element 1 and 2. l_{ij} is the length of the boundary between the element 1 and 2.

For the stationary field, the tangential and normal (radial) components of the local force density can be obtained by

$$f_t = -I_m B_n^{ext} = -\frac{1}{\mu_0}(B_{1t}-B_{2t})\frac{B_{1n}+B_{2n}}{2} \qquad (2)$$

$$f_n = I_m B_t^{ext} = \frac{1}{\mu_0}(B_{1t}-B_{2t})\frac{B_{1t}+B_{2t}}{2} \qquad (3)$$

where superscript *ext* implies the external field, subscript *n* and *t* imply the normal component and tangential component, respectively. .

The experiment current waveforms are used to calculate the tangential and normal components of the local force and shown in Fig. 6. The waveforms of the calculated local forces are shown in Fig. 7. It can be seen that the tangential forces of these two models have the similar peak and mean values due to their equal torque.

IV. Modal Analysis and Deformation Analysis

Based on the principle of Hamilton, the modal analysis can be descriped in (4) with considering the undamping system and external force free

$$[M]\{\ddot{x}\}+[K]\{x\}=0 \qquad (4)$$

where x is the vector of the displacement, $[M]$ is the mass matrix, and $[K]$ is the stiffness matrix. When estimate the vibration, the deformation analysis requires to consider both

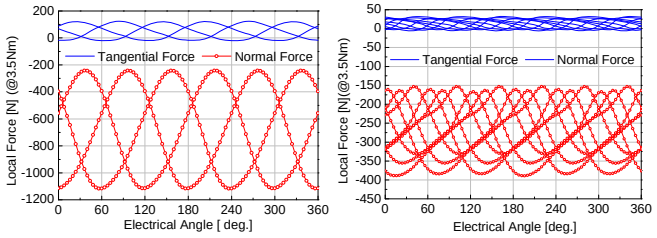

(a) (b)

Fig. 7. Calculated local forces of the study models: (a) 8-pole/12-slot model; (b) 8-pole/9-slot model.

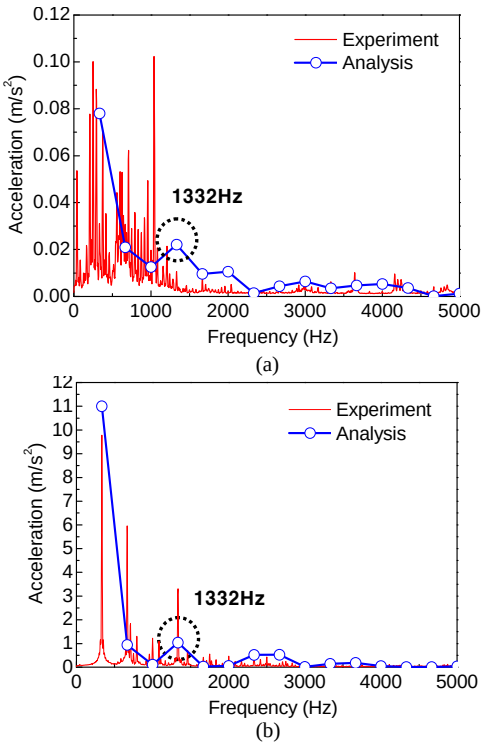

(a)

(b)

Fig. 8. Comparison of analysis and experiment results of vibration: (a) 8-pole and 12-slot model; (b) 8-pole and 9-slot model.

TABLE II
COMPARISON OF ANALYSIS AND EXPERIMENT RESULTS @2500RPM

Item		8-pole/12-slot	8-pole/9-slot
Peak value [m/s^2]	Analysis	0.078	11.03
	Experiment	0.088	9.77
Frequency [Hz]	Analysis	333	333
	Experiment	290	334

the damping and applied force vector. Thus, the mechanical system is expressed as (5).

$$[M]\{\ddot{x}\}+[C]\{\dot{x}\}+[K]\{x\}=\{F(t)\} \tag{5}$$

where $[C]$ is the damping matrix and $\{F(t)\}$ is the applied force vector [5]. In this study, the vector $F(t)$ only consists of the harmonic components of the calculated local force, because the DC component has no effect on the vibration. Fig. 8 (a) and (b) show the calculated vibrations of these two motors at 2500rpm and 3.5Nm output torque, respectively.

V. HARMONIC ANALYSIS OF VIBRATION

In the harmonic analysis using the electromagnetic force F as an example, first of all, the k-th space harmonic component is separated from the field analysis result as a function of the circumferential position x_s of the stator coordinate at each time t in the field analysis. The separated electromagnetic force $F_t(x_s)$ can be expressed as follows [7].

$$F_t(x_s)=\sum_k F_k \sin(kx_s+\alpha_k) \tag{6}$$

Where F_k is the amplitude of the k-th space harmonic components, and α_k is the phase angle. Equation (6) means only space harmonic components at each time-step.

Next, the v-th time harmonic component is separated from the k-th space harmonic component at every circumferential position x_s of the stator coordinate. The separated harmonic component $F_{ks}(l)$ is presented as follows.

$$F_{kx}(t)=\sum_k F_{kv} \sin(v\omega t+\alpha_{kv}) \tag{7}$$

where ω is the electrical angular frequency, F_{kv} is the amplitude of the v-th time for the k-th space harmonic components, and is the phase angle. In the proposed method, each harmonic component is separated into positive-phase-sequence and negative-phase-sequence harmonic waves which are functions of the circumferential position x_s and time t.

At the two circumferential positions x_{s1} and x_{s2} of the stator coordinate, the v-th time, for the k-th space harmonic electromagnetic force F_{kvl} and F_{kv2} are given as follows.

$$\begin{aligned}&F_{kv1}\sin(v\omega t+\alpha_{kv1})\\&=F_{kvp}\sin(v\omega t-kx_{s1}+\alpha_{kvp})+F_{kvn}\sin(v\omega t+kx_{s1}+\alpha_{kvn})\end{aligned} \tag{8}$$

$$\begin{aligned}&F_{kv2}\sin(v\omega t+\alpha_{kv2})\\&=F_{kvp}\sin(v\omega t-kx_{s2}+\alpha_{kvp})+F_{kvn}\sin(v\omega t+kx_{s2}+\alpha_{kvn})\end{aligned} \tag{9}$$

where α_{kv1} and α_{kv2} are the phase angles of F_{kvl} and F_{kv2}, respectively; F_{kvp} and F_{kvn} are the amplitudes of the positive-phase-sequence and negative-phase-sequence v-th time for the k-th space harmonic components, respectively; α_{kvp} and α_{kvn} are the phase angles of the positive-phase-sequence and negative-phase-sequence v-th time for the k-th space harmonic components, respectively. By solving (8) and (9) simultaneously, the amplitudes and the phase angles of the positive-phase-sequence and negative-phase-sequence harmonic components can be obtained. In this process, the circumferential positions x_{s1} and x_{s2} are chosen where each absolute value of the harmonic amplitude by (7) is the maximum or minimum, though any position can be chosen freely.

Consequently, the electromagnetic force $F(x_s,t)$ by the above FEM analysis can be expressed as (10).

$$\begin{aligned}F(x_s,t)=\sum_k\sum_v[&F_{kvp}\sin(kx_s-v\omega t+\alpha_{kvp})\\&+F_{kvn}\sin(kx_s+v\omega t+\alpha_{kvn})]\end{aligned} \tag{10}$$

VI. EXPERIMENT VERIFICATION AND ANALYSIS

Before the vibration test, the natural frequencies of these two motor are verified by modal test. Due to thick and stiff

housing, the natural frequencies of both motors on mode 2 are about 1280Hz. Fig. 9 shows the experiment system for testing the vibration. This system is solely set in a sound proof chamber. The operation condition of experiment is same to that of analysis, i.e. 2500rpm and 3.5Nm load torque. The measured vibrations of these two motors are compared with the analysis results as shown in Fig. 8. Although there are differences on the some harmonic orders, the total trend and peak values of the analysis results are almost same to the experiment results. The peak value and frequency of the analysis and experiment vibration results are compared in Table II. It can be seen that the peak value of vibration in the 8-pole/9-slot achieves about 110 times of the 8-pole/12-slot. It should be noted that there is the other peak value of vibration which does not appear in analysis results in Fig. 8 (a). In fact, this is because of the different scales in Fig. 8 (a) and (b). This kind of vibration also exists in 8-pole/9-slot motor, which may be caused by the slight eccentricity of manufacture, torque pulsations, or the reduction gears. In addition, measured vibrations of these two motors are compared with the harmonic analysis results in Fig. 10. The tendency of the results is similar to the result in deformation analysis results. Two points of view can be applied and the first one is that the peak value occurred in 333Hz which is the fundamental frequency of electromagnetic force generated by 8 poles motor at 2500rpm. The harmonic components of integer multiple of the fundamental frequency are electromagnetic force. The second point of view is that the natural frequencies of these two motor are about 1280Hz, therefore the amplitude of 1332Hz is remarkable for it's great value compared to the other harmonic orders in Fig 8. The effect of electromagnetic forces increased due to the correspondence between components of natural frequencies and electromagnetic forces.

VII. Conclusion

Two PMSM's are compared in this paper for revealing the effect of the combination of pole and slot on the vibration. According to the harmonic analysis of the radial force it is found that the number of slot which is the integral multiple of the harmonic components of the rotor pole is preferred in order to avoid the low harmonic radial force and reduce vibration. Additionally, an analysis process for predicting the vibration of motor and an experiment verification method are introduced. The validation of the analysis methods on the vibration in this paper is verified by this experiment.

References

[1] Z. Q. Zhu, Z. P. Xia. L. J. Wu and G. W. Jewell, "Analytical Modeling and Finite-Element Computation of Radial Vibration Force in Fractional-Slot Permanent-Magnet Brushless Machines," *IEEE Trans. on Magn.*, vol.46, no.5, pp. 1908-1918, 2010.

[2] J. P. Hong and K. H. Ha, "Stator Pole and Yoke Design for Vibration Reduction of Switched Reluctance Motor," *IEEE Trans. on Magn.*, vol.38, no.2, pp. 1-4, 2002.

[3] L. Vandevelde and J. A. A. Melkebeek, "A Survey of Magnetic Force Distributions Based on Different Magnetization Models and on the Virtual Work Principle," *IEEE Trans. on Magn.*, vol.37, no.5, pp. 3405-3409, 2001.

[4] Y. S. Chen, Z. Q. Zhu and D. Howe, "Vibration of PM Brushless Machines Having a Fractional Number of Slots Per Pole," *IEEE Trans. on Magn.*, vol.42, no.10, pp. 3395-3397, 2006.

[5] S. H. Lee, J. P. Hong, S. M. Hwang, W. T. Lee, etc., "Optimal Design for Noise Reduction in Interior Permanent-Magnet Motor," *IEEE Trans. on Magn.*, vol.45, no.6, pp. 1954-1960, 2009.

[6] G. Henneberger, Ph. K. Sattler and D. Shen, "Nature of the Equivalent Magnetizing Current for the Force Calculation," *IEEE Trans. on Magn.*, vol.28, no.2, pp. 1068-1071, 1992.

[7] H. Mikami, K. Ide, K. Arai, M. Takahashi and K. Kajiwara, "Dynamic Harmonic Field Analysis of an Inverter-Fed Induction Motor Considering All Harmonic Components in the Secondary Current," IEEE-IAS, Conf. Rec. 1995, pp 579-583

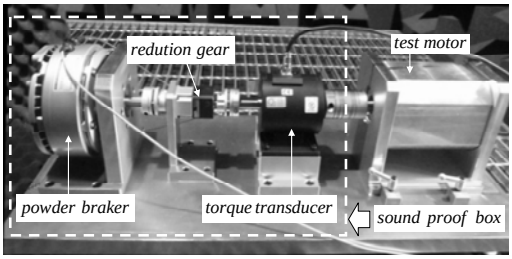

Fig. 9. Experiment system for testing the vibration

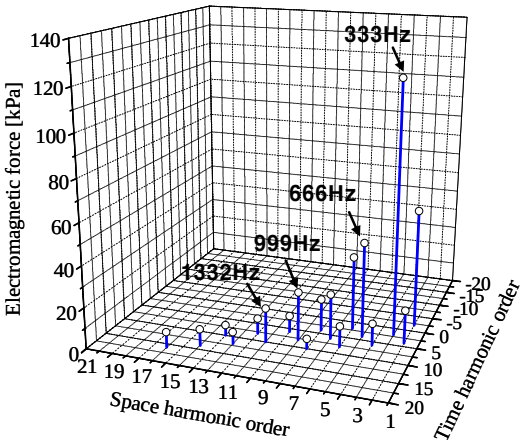

(a) 8pole / 12slot

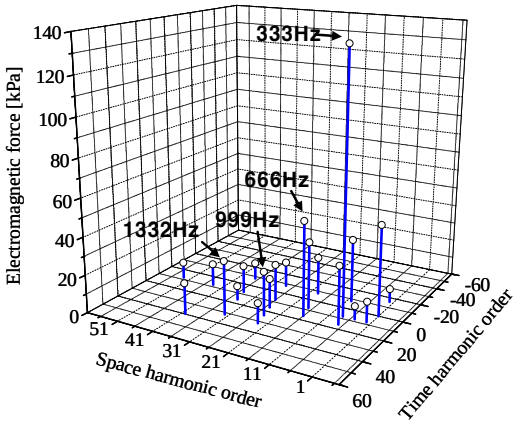

(b) 8pole / 9slot

Fig. 10. Spectrum analysis according to number of pole and slot